Check for updates

OPEN ACCESS

DOI: 10.46903/gjms/22.02.1640

ORIGINAL ARTICLE

MOLECULAR DOCKING, ADMET, AND MOLECULAR DYNAMICS SIMULATION STUDIES FOR MOLECULES WITH EXPECTED HDAC INHIBITION ACTIVITY

Zaid Mahmood Mohammed[1], Ayad Abed Ali Al-Hamashi[2]

[1]Babylon Health Directorate, Ministry of Health, Iraq, [2]Department of Pharmaceutical Chemistry, College of Pharmacy, University of Baghdad, Iraq

ABSTRACT

Background: Histone deacetylases (HDACs) are promising epigenetic target for the treatment of a variety of diseases including cancer, inflammations, and neurological disorders. A number of. HDAC inhibitors have been approved for the treatment of cancer. Most of the HDAC inhibitors have poor pharmacokinetic properties such as short half-life, fast metabolism, and clearance. To overcome this limitation, several attempts are ongoing to develop new molecules with unique zinc binding groups. The objective is to design and evaluate new compounds featuring heterocyclic ring-based zinc binding groups (ZBGs) targeting histone deacetylases (HDACs) for potential therapeutic use in various diseases, including cancer, inflammations, and neurological disorders. The expected zinc chelation activity for ZBG in addition the construction of the linker and the cap group were evaluated using molecular modeling studies.

Materials & Methods: A series of new compounds with promising HDAC inhibition activities were designed based on a molecular modeling to improve the HDACs inhibitory potency, improving pharmacokinetic properties, and conferring cancer cell targeting. Twenty new compounds (K1-K20) were designed via special modification of common structural activity relationship (SAR) of HDAC inhibitors using heterocyclic rings as a zinc binding group (ZBG), diverse group in cap group, and hydrophobic linker. These compounds were analyzed by docking study, ADMET, and molecular dynamics (MD) simulations against HDAC isoforms using vorinostat as a reference.

Results: The docking study revealed that the proposed compounds haves higher docking score than vorinostat. All molecules were showed promising virtual HDACs binding affinity. The ADMET analysis of the designed compound showed acceptable pharmacokinetics results. In comparison to vorinostat, the MD simulation analysis revealed that compound K1 had significantly perfect alignment to HDAC8.

Conclusions: The precise virtual binding affinity for K1 might be attributed to the unique chelation capacity of the amino group of imidazole ZBG of K1 with zinc metal cofactor of HDACs enzymes, other interaction of linker with surrounding amino acid residues, and the presence of fused aromatic ring in cap group.

KEY WORDS: HDAC8; Vorinostat; Molecular docking; ADMET; Molecular dynamic.

Cite as: Mohammed ZM , Al-Hamashi AAA. Molecular docking, ADMET and molecular dynamics simulation studies for molecules with expected HDAC inhibition activity. Gomal J Med Sci 2024 Apr-Jun;22(2):164-72. https://doi.org/1046903/gjms/22.02.1640

1. INTRODUCTION

The term "epigenetics" describes a genomic process that reversibly alters gene expression without altering DNA sequences.[1] Epigenetic dysregulation is highly correlated with human disease, including cancer.[2] Targeting epigenetic dysregulation is a useful strategy for tackling diseases.[3] Histone epigenetic modification is a vital target the development of novel medications, including histone deacetylase (HDAC) inhibitors.[4,5] Three primary pharmacophoric moieties building the HDAC inhibitors structure: a hydrophobic linker, a zinc binding group (ZBG), and a surface recognition moiety, which is called the "cap" unit.[6] Some of these inhibitors get an approval by American food and drug administration (FDA) for treatment of cutaneous T-cell lymphoma (CTCL), Multiple Myelo-

Corresponding Author:

Dr. Ayad Abed Ali Al-Hamashi
Department of Pharmaceutical Chemistry
College of Pharmacy
University of Baghdad, Iraq
E-mail: a.alhamashi@copharm.uobaghdad.edu.iq

Date Submitted: 24-04-2023
Date Revised: 15-11-2023
Date Accepted: 26-01-2024

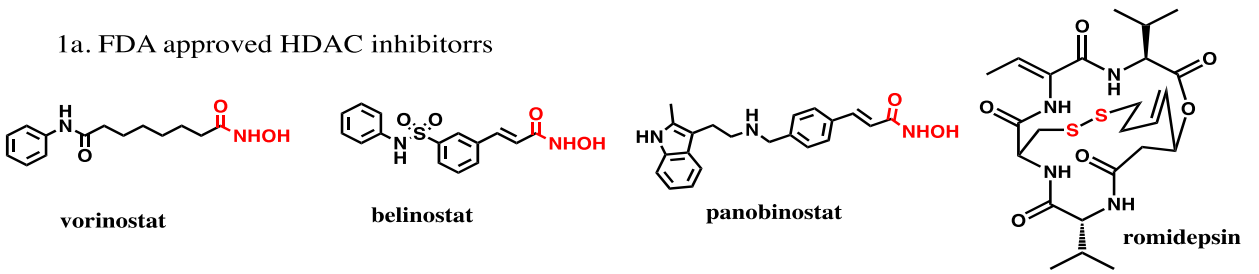

Figure 1: The FDA approved HDAC inhibitors

ma (MM) and peripheral T-cell lymphoma (PTCL) such as romidepsin, vorinostat, belinostat, and panobinostat are FDA approved HDAC inhibitors, whereas chidamide obtain an approval by Chinese Food and Drug Administration (CFDA) for acute myeloid leukemia (Figure 1).[7] HDAC inhibitors have many drawbacks such as off-target toxicities and poor pharmacokinetic properties.[8] HDAC inhibitors are either used alone or in conjunction with other antiproliferative agents to treat cancer. Hence, the developing of HDAC inhibitor with optimum selectivity, potency, and pharmacokinetic properties is an optimum goal to be achieved.

Over the last few decades, molecular modeling has become fastest developing fields due to various structural requirements in drug discovery and remarkable increase in the availability and capability of computers power. The molecular modeling studies are improving the drug discovery processes by the prediction of binding affinity of the biologically active molecules into molecular targets.[9-11] A number of computer programs are utilized for molecular docking, including AutoDock vina, Glide, FlexX, MOE, FRED, and GOLD. In this study we are designing new HDAC inhibitors containing heterocyclic moiety as new ZBG with decent virtual binding affinity and pharmacokinetic profile by using glide software from Schrödinger company. Hence, in this work we employed the molecular modeling tools to design new HDAC inhibitor with accepted predicted selectivity, potency, and pharmacokinetic properties

2. MATERIALS AND METHODS

2.1. Docking Study:

The Docking study was performed using a licensed Glide program embedded within the maestro software from Schrodinger's modeling suite (version 13.013) [12]. The docking process consist of three main steps starting with protein preparation, ligand construction, and grid generation. The crystal structure of HDAC6 (PDB ID: 5EDU), HDAC2 (PDB ID: 4LXZ) and HDAC8 (PDB ID: 1T69) proteins was downloaded from protein data bank (PDB)[13-15]. The protein was prepared using the default setup as the bond order were assigned, hydrogens were added, the missing loops of protein were filled, water molecules that are not involve in interaction (beyond 5 Å from het group) and non-essential atoms were deleted. The presence of zinc ion in these proteins as co-factor provide bidentate or monodentate interaction with ZBG of ligands. The receptor grids were generated using the ligand as center for the boundary box where the ligands docked in binding site of protein. The size of grid box for optimal interaction was (X: 10 Å, Y: 10 Å and Z: 10 Å).[16] Ligands were prepared through LigPrep wizard (Schrödinger Release 2023-4: LigPrep, Schrödinger, LLC, New York, NY, 2023). All ligands in workspace were either sketched inside the software or imported from files drawing by chemdraw program version 18.0.0.23. The small library was obtained either from the binding database or by the modification in one part of het ligand by enumeration order inside the software. Vorinostat was used as a reference compound. The selected ligands energy was minimized by the applying of the force fields (OPLS5) to generate 5 poses per ligand.[17] Finally, the molecular docking experiment for the prepared ligands and the prepared protein were performed using the extra precision (XP) docking mode. The docked ligands were ranked according to glide docking score (G score), potential energy predictions, and ligand binding geometries.[18]

2.2. ADME Study:

The pharmacokinetic properties including the intestinal absorption, systemic distribution, metabolism, excretion, and toxicity can be also identified virtually by ligand based ADME prediction using Qikprobe software in Schrodinger maestro. The setting includes opening the Qikprobe panel to insert all entries from project table of docking compounds, then chose the fast mode for ADMET analysis, and then running QikProp in fast processing mode, compounds with acceptable docking score and fitness to the receptors, and compatible with Lipinski's rule of five were nominated for molecular dynamic simulation evaluation.[19]

2.3. Molecular Dynamics Simulation:

The molecular dynamic (MD) simulation was conducted using Desmond module version 2.0[20], as the top-ranked compounds from the docking study were selected for the MD simulation study to evaluate the long of ligand binding persistence into the pocket of protein. The system was built up by choosing a SPC

water model in the boundary box of three dimension (10 Å * 10 A° * 10 Å). The ions (Na^+ and Cl) or salt were added, as the software detected the number of ions to be added at neutral PH. The MD simulations time was selected over 50 nanoseconds (ns) and recording interval time of 100 picosecond (ps) with about 100 frames for each simulation at a constant temperature of 300 K and pressure at 1 bar.[21] The root means square deviation (RMSD) and the root means square fluctuation (RSMF) were plotted versus time to conclude the alignment.

3. RESULTS

3.1. Molecular Docking Study:

The design compound's structure was inspired from the vorinostat scaffold with the replacement of the hydroxamate ZBG by a heterocyclic ring. The cap group is also exchanged with various substituted aromatic moieties, and the availability of aromatic linker to enhance the binding affinity into the active site.

A library of ~2700 compounds was obtained from modification on the pharmacophoric moiety of vorinostat (ZBG, the cap, and the linker), and further modification through enumeration of possible atoms in the ZBG by enumeration tool in maestro software to obtain ~2700 ligands. All molecules were docked through the high-throughput virtual screening (HTVS) against crystal structures of homosapien HDAC6 (PDB ID: 5EDU), HDAC2 (PDB ID: 4LXZ), and HDAC8 (PDB ID: 1T69). The top compounds which interact with HADC2, HADC6, and HADC8 proteins for reasonable affinity with docking score better than -5 kcal/mole (150 compounds) have been selected for second docking run using SP docking[22]. Then, compounds with threshold energy higher than -7 kcal/mole (50 compounds) from SP docking were nominated to the third run of docking study using extra precise (XP) docking (Table 1). Finally, top twenty compounds that have higher docking score with a proper interaction fitness into the receptor active site were selected for the pharmacokinetic (ADME) properties evaluation (Figure 2).

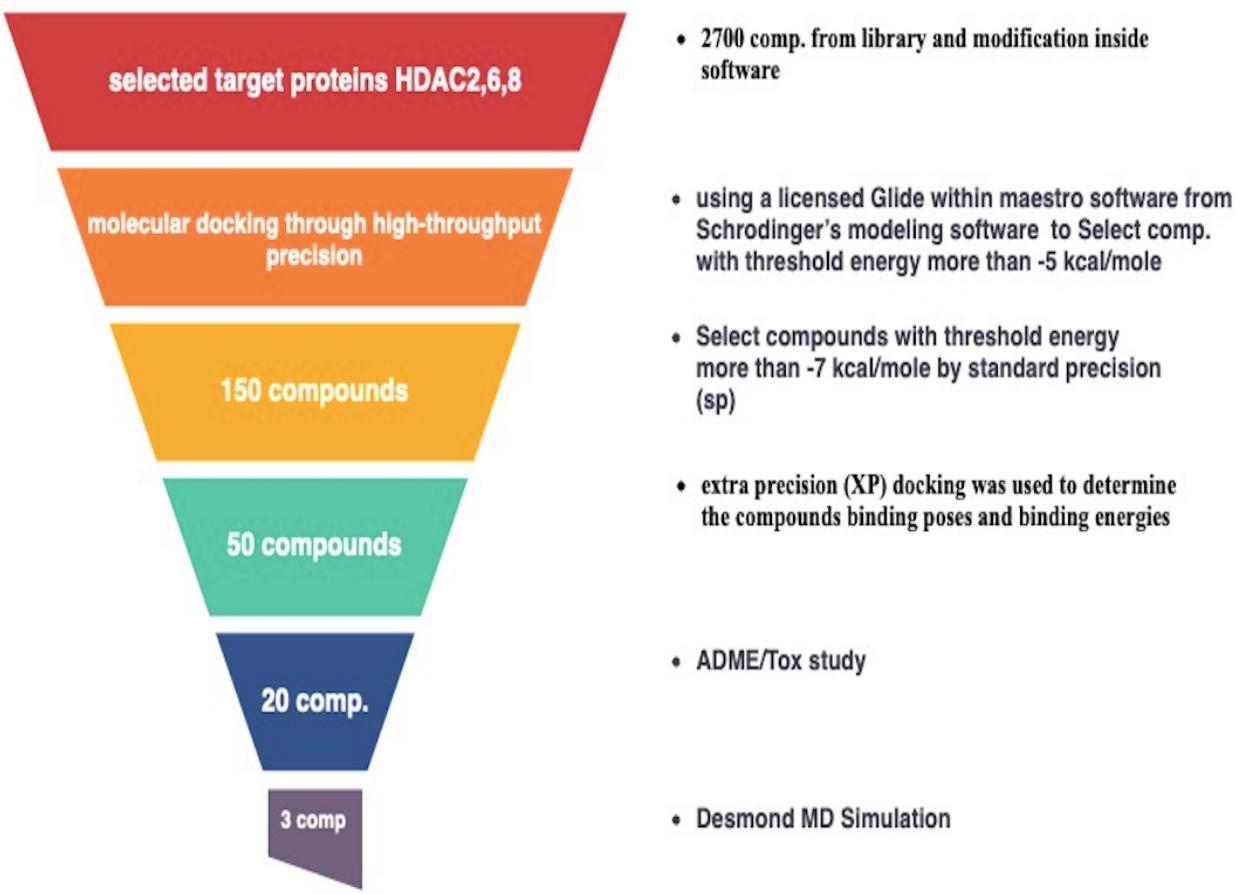

Figure 2: The protocol for the molecular modeling studies

Table 1: Docking score of proposed compounds on various HDACs protein

Comp. I	Comp name	Docking score		
		HDAC 2 4LXZ	HDAC 6 5EDU	HDAC 8 1T69
K1	4-((1H-benzo[d]imidazol-2-yl)amino)-N-(1H-imidazol-2-yl)benzamide	--9.71	-10.55	-10.15
K2	N-(1H-imidazol-2-yl)-4-(quinolin-6-ylamino)benzamide	-9.61	-10.34	-10.12
K3	N-(4-((1H-imidazol-2-yl)carbamoyl)phenyl)-4-((pyridin-3-yloxy)methyl)benzamide	-8.63	-10.36	-9.78
K4	N-(4-((1H-imidazol-2-yl)carbamoyl)phenyl)-4-methoxybenzamide	-9.45	-10.25	-8.88
K5	N-(4-((1H-imidazol-2-yl)carbamoyl)phenyl)-4-(3-chlorophenyl)-2,3-dihydro-1H-pyrazole-3-carboxamide	-8.86	-9.42	-9.08
K6	(E)-4-(phenyldiazenyl)-N-(1H-1,2,4-triazol-3-yl) benzamide	-9.33	-9.44	-8.70
K7	N-(4-(oxazol-2-ylcarbamoyl)phenyl)-6-phenylpyrimidine-4-carboxamide	-9.24	-9.35	-9.52
K8	N-(4-(furan-2-ylcarbamoyl)phenyl)-3,4-dihydrocinnoline-1(2H)-carboxamide	-9.56	-9.25	-9.72
K9	N1-(3-amino-5-hydroxyphenyl)-N4-(4-(oxazol-2-ylcarbamoyl)phenyl)terephthalamide	-10.31	-9.18	-9.59
K10	(E)-4-((pyridin-2-ylimino)methyl)-N-(1H-1,2,4-triazol-3-yl) benzamide	-8.62	-9.54	-8.29
K11	(E)-4-(((2,3-dihydro-1H-inden-5-yl)imino)methyl)-N-(1H-1,2,4-triazol-3-yl)benzamide	-8.504	-9.18	-8.34
K12	(E)-4-((thiazol-2-ylimino)methyl)-N-(1H-1,2,4-triazol-3-yl) benzamide	-8.506	-9.15	-8.54
K13	(E)-4-((phenylimino)methyl)-N-(1H-1,2,4-triazol-3-yl) benzamide	-8.54	-9.35	-8.47
K14	(E)-4-((p-tolylimino)methyl)-N-(1H-1,2,4-triazol-3-yl) benzamide	-8.55	-9.20	-8.46
K15	(E)-4-((naphthalen-2-ylimino)methyl)-N-(1H-1,2,4-triazol-3-yl)benzamide	-8.6	-9.52	-8.32
K16	(E)-4-(((4-bromophenyl)imino)methyl)-N-(1H-1,2,4-triazol-3-yl)benzamide	-7.81	-7.31	-7.62
K17	(E)-4-(((4-methoxyphenyl)imino)methyl)-N-(1H-1,2,4-triazol-3-yl)benzamide	-8.57	-8.62	-6.77
K18	(E)-4-(3-oxo-3-phenylprop-1-en-1-yl)-N-(1H-1,2,4-triazol-3-yl)benzamide	-8.24	-8.62	-8.67
K19	(E)-4-(3-(4-aminophenyl)-3-oxoprop-1-en-1-yl)-N-(1H-1,2,4-triazol-3-yl)benzamide	-8.23	-8.71	-8.12
K20	(E)-4-(3-(4-chlorophenyl)-3-oxoprop-1-en-1-yl)-N-(1H-1,2,4-triazol-3-yl)benzamide	-8.61	-8.75	-8.65
Ref.	Vorinostat	-7.57	-9.1	-9,107

3.2. ADME Study:

The ADME results showed that the top-ranking compounds have no violation to Lipinski rule of five or rule of three, which assigns them as possible drug-like molecules. The top-ranking compounds showed less possible CNS penetration with good oral bioavailability, also from QPPCaco (model for gut-blood barrier) compounds **K2** and **K8** has great permeability (value >500 nm/sec. consider great and <25 consider poor) while other tested compound show acceptable permeability. Finally, from number of likely metabolic reactions (#Metab) the results showed all compounds have no structure labiality to undergo other metabolic reaction as aromatic OH oxidation, enol oxidation and other (normal range 1-8)[23].

3.3. Molecular Dynamic Simulation Study:

The nature of the ligand-target interaction is dynamic. Therefore, the MD simulation studies are applied to evaluate the viability of the virtual interaction between ligand and target.[24] In this study, the highest-scoring ligand (**K1**) with the most significant drug-like properties, and lowest-scoring ligand (**K13**) were chosen. MD simulations were applied to these compounds to understand the evolution of receptor binding ability over time. In particular, we examined the dynamic interaction profile of the ligand with important residues that can affect their occupancy and activity in the protein binding pocket.

Table 2: Drug likeness properties for the top-ranking molecules.

Comp ID	M WT	Rule of 5	Rule of 3	Oral absorption	Donor HB	AccpHB	#Metab	CNS	QPPCaco
K1	318	0	0	3	3	5	0	-2	363.5
K2	371	0	0	3	2	5	2	-2	535.4
K3	418	0	0	3	2	6.25	4	-2	237.2
K4	322	0	0	3	2	6.25	1	-2	410.8
K5	408	0	0	2	4	9	1	-2	31.4
K6	292	0	0	3	2	7.5	1	-2	327
K7	385	0	0	2	4	9	3	-1	387.3
K8	364	0	0	3	3	6	4	-2	643.5
K9	457	0	0	3	5.5	9	4	-2	45
K10	306	0	0	3	2	7.5	1	-2	301.66
K11	298	0	0	3	2	8	0	-2	473.6
K12	335	0	0	3	2	8	1	-2	266.5
K13	291	0	0	3	2	6.5	0	-2	473.6
K14	305	0	0	3	1	5	1	-2	470.9
K15	341	0	0	3	2	6.5	0	-2	471.2
K16	370	0	0	3	2	6.5	0	-2	155.2
K17	321	0	0	3	2	7.25	1	-2	471.5
K18	318	0	0	3	2	7.5	0	-2	155.8
K19	333	0	0	3	3.5	8.5	1	-2	45.27
K20	353	0	0	3	2	7.5	0	-2	176.3
vorinostat	264	0	0	3	3	6.7	3	-2	138.13

Lipinski Rule include mol_MW < 500, log p < 5, HBD ≤ 5, HBA ≤ 10. (Limit 0-3 obey this rule)

Rule Of Three (Gorgensen's rule): P log > -5.7, QP PCaco > 22 nm/s, Primary Metabolites < 7 (Limit 0-3 obey this rule)

Human Oral Absorp. limit 1 for low, 2 for medium and 3 for high absorption.

CNS: Predict activity of central nervous system in scale of –2 (inactive) and +2 (active)

Gut-blood barrier QP PCaco < 25 poor permeability, >500 great.

3.3.1. Protein- ligand RMSD value (PL-RMSD):

Comparing the compound **K1-**1T69 complex, **K13-**1T69 complex to the vorinostat-1T69 complex over simulation time of 50 ns. The result showed that compound **K1-**1T69 complex has ligand RMSD value of (1.25-1.6 Å) and the RMSD value for 1T69 protein is (1.5-1.8 Å) (Figure 3-A). For **K13**-1T69 complex the ligand RMSD value is 1.2-1.6 Å and for 1T69 protein is **(**1.8-3.6 Å) (Figure 3-B). While for vorinostat**-**1T69, RMSD value for 1T69 protein range (1-1.4 Å) and for vorinostat (3-6 Å) (Figure 3-C). Results were showed that during the simulation period, the ligand aligned with the protein and underwent comparable conformational changes. The MD result also showed that the interaction stability for **K1-**1T69 complex is higher than vorinostat and **K13.**

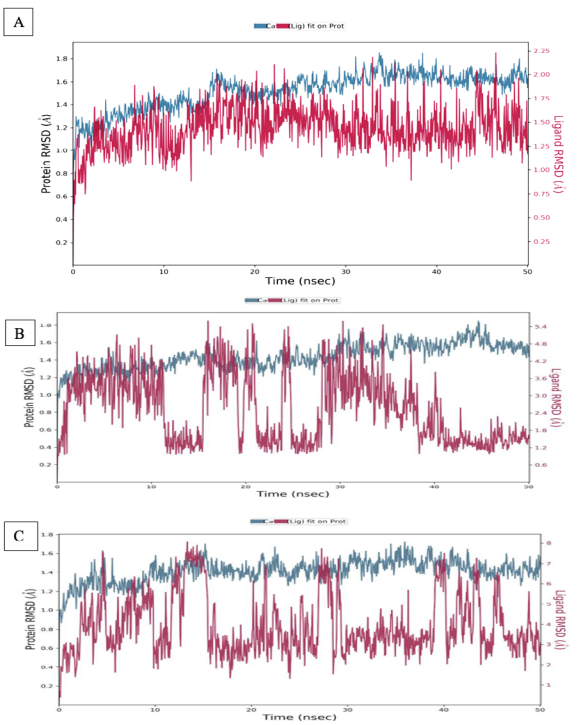

Figure 3: RMSD values in versus time for (A) k1-1T69, (B) k13-1T69 complex, and (C) vorinostat-1T69.

3.3.2. Ligand RMSF (L-RMSF):

The root mean square fluctuation for ligand (L-RMSF) is helpful in describing modifications to the positions of the ligand atoms. The ligand RMSF, which corresponds to the 2D structure in the top panel, displays the ligand's fluctuations broken down by atom. The ligand RMSF may provide an insight on interaction of ligand binding groups with binding pocket of protein and their entropic participation in the binding event. In the bottom panel, the fluctuations of the ligand in relation to the protein are displayed on the 'Fit Ligand on Protein' line. Prior to measuring the ligand RMSF on the ligand heavy atoms, the protein-ligand complex is first aligned on the protein backbone as shown in figure 4 (L-RMSF) of compound **K1** (1-0.5 Å) demonstrates perfect fitting of the ligand along simulation time over 25 atoms with the protein if we compare this result with more fluctuations in L-RMSF of **K13** (3.5- 0.5) and L-RMSF of vorinostat with (5-0.5 Å) (Figure 4).

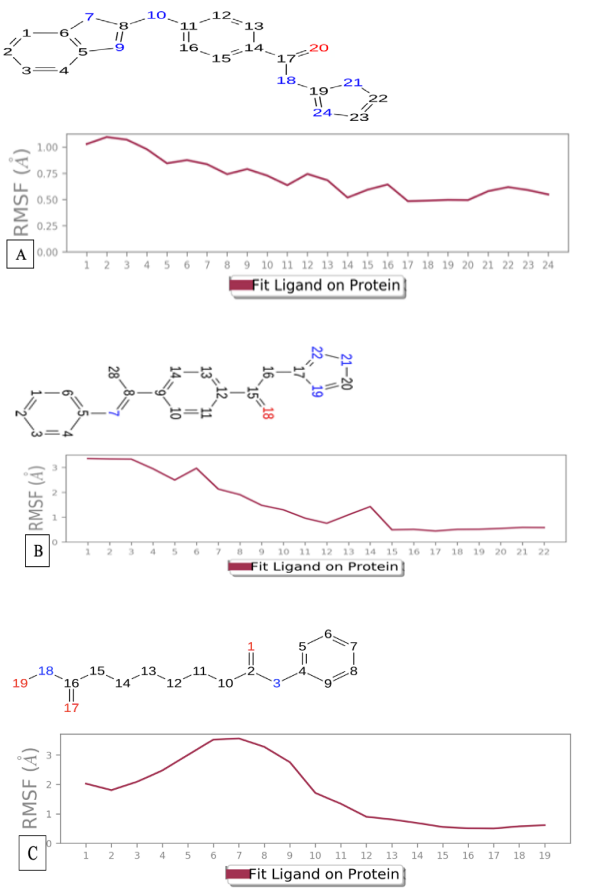

Figure 4: L-RMSF value for (A) K1-1T69 complex, (B) K13-1T69 complex, and (C) vorinostat-1T69 complex.

3.3.3. Protein-RMSF (P-RMSF):

The P-RMSF is indicating the regions of the protein that fluctuate more when the simulation runs. More fluctuations are seen in the protein's tails (N- and C-terminal) than in any other region. Compared to the unstructured portion of the protein, secondary structural elements such as alpha helices and beta strands are typically more rigid and fluctuate less than loop sections. On these plots above, show P-RMSF value for complex **K1**-1T69 less than 1 Å (normal value less than 1 Å) while p-RMSF value for vorinostat and **K13**-1T69 complex show some amino acid fluctuation near 1.2 Å. Vertical bars that are colored green indicate protein residues that have interactions with the ligand. (Figure 5).

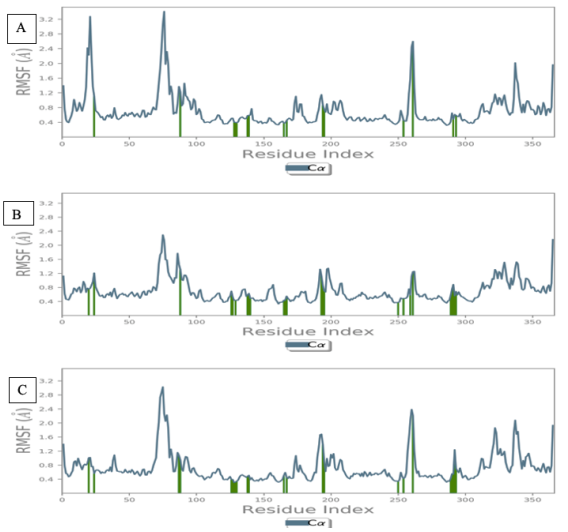

Figure 5: P-RMSF value for (A) K1-1T69 complex, (B) K13-1T69 complex and (C) vorinostat-1T69 complex.

3.3.4. Protein-Ligand Contacts:

The MD analysis can provide an idea about the stability of various ligand-protein interactions (ionic, hydrophobic, H-bonds and water bridges). The panel displays the total number of distinct contacts that the protein has during the trajectory with the ligand. The active site amino acids participate in the interactions is GLY-151 and HIS-142 bind with comp **k1** through hydrogen bond interaction. The π-π interaction through HIS-143, metal coordination through ASP-178, ASP-276 and HIS-180. The strength of interaction of HIS and ASP is 100% with zinc ion (Figure 6). An illustration of the complex interactions between ligand atoms and protein residues interactions that take place in the chosen trajectory (0.00 to 50.05 ns) for more than 30.0% of the simulation time, as depicted in (Figure 6)

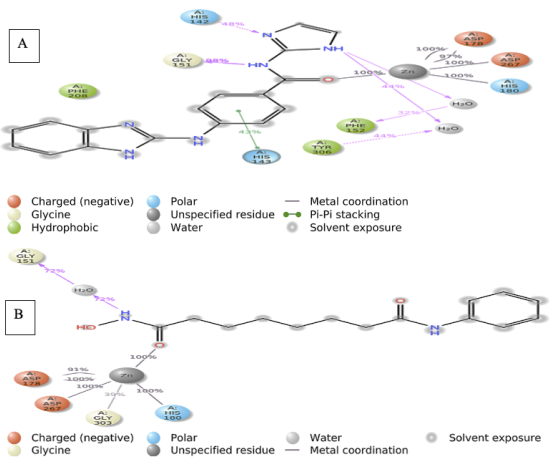

Figure 6: The interaction of comp. K1 and vorinostat with 1T69 protein

The above panel shows which residues interact with the **K1** in each trajectory frame, for example, strong interaction noticed between carbonyl group and zinc ion through metal coordination (100%), amino group of imidazole ring also made interaction through H-bond with essential water bridge and PHE-152 and TYR-306 (32 and 44% respectively), NH-amide group with GLY-151 through H-bond (98%), N-heteroatom of imidazole through H-bond with HIS-142(48%) and Pi-Pi stacking interaction through aromatic ring with HIS-143 (43%). These various interactions provide perfect induce-fit between **K1** and 1T69 along simulation time and prevent **K1** compound to dissociate out from active site. In comparison to the reference compound vorinostat with less various interaction (H-bonding between NH-group of ZBG hydroxamic acid with GLY-151 residue and metal coordination between carbonyl group and zinc metal ion).

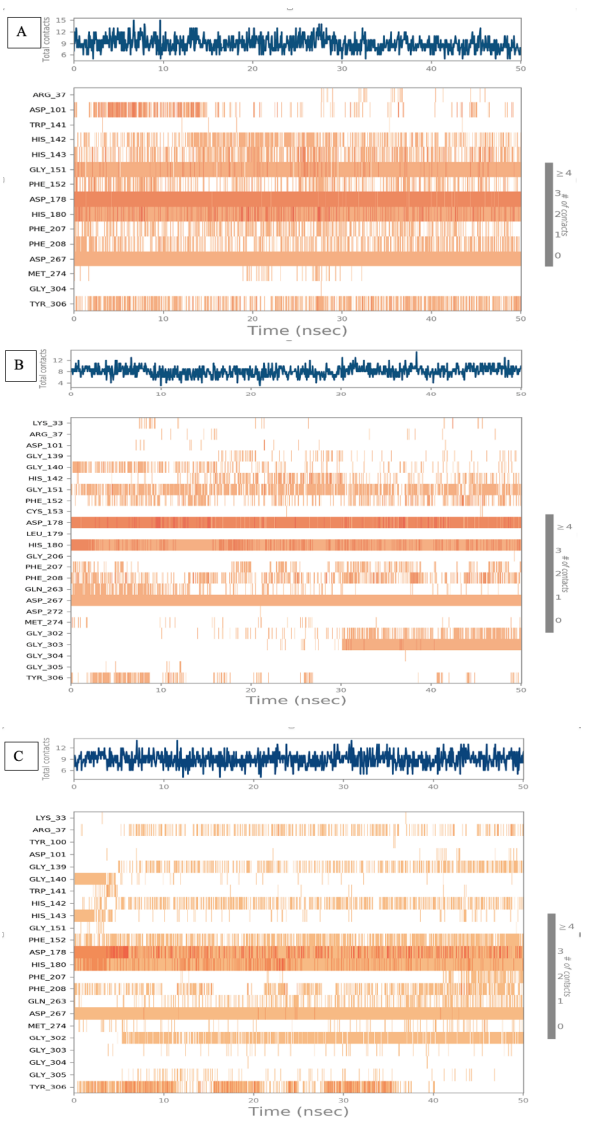

Figure 7. Protein-Ligand Contacts of (A) compound k1-1T69 complex, (B) for vorinostat and (C) for compound k13-1T69 complex

The scale to the right of the plot indicates that certain residues make multiple specific contacts with the ligand, which is represented by a dark orange area. For example, in **K1-**1T69 complex there is strong contact between compound **K1** and GLY-151, ASP-178, HIS-180 and ASP-267 amino acid residues. While ASP-178, HIS-180 and ASP-267 amino acid contact strongly with vorinostat in vorinostat-IT69 complex.

4. DISCUSSION

From molecular docking study, compound **K1** have higher docking score against selected isoforms of HDACs with a proper interaction fitness into the enzyme active site through bidentate interaction between carbonyl group of amide and primary amine group of imidazole ring as ZBG. These interactions provide electrostatic complementarity inside the active site of HDACs enzymes in addition to geometrical complementarity that provide an imagination about ligand protein interaction stability. To validate the virtual interaction of compound **K1** inside the active site and not dissociate out, compound **K1** was subjected to the MD simulation studies. The MD simulation parameters of PL-RMSD, P-RMSF, L-RMSF, and PL-contact indicating a perfect alignment in **K1**-1T69 complex and minimal fluctuation along simulation time. Also, from the ADME results comp. **K1** showed accepted pharmacokinetic properties to be dru-like molecule. It is not violating Lipinski rule of five or Jorgensen's rule of three, with less CNS penetration, good oral bioavailability and good permeability that allows it to overcome main drawbacks associated with pharmacokinetic profile of FDA approved HDACIs.

5. CONCLUSION

In this work we tried to virtually study new HDAC inhibitors. The generated library was structurally inspired from the structure of vorinostat. Our docking procedure was started by a high-throughput virtual screening (HTVS)for ~2700 compounds, which followed by more precise docking experiments to reach molecules having superior potential molecules. The top-ranking compounds were thoroughly studied by ADMET study and molecular dynamic simulation. The most promising molecule **K1** has imidazole ring as ZBG connect through amide linkage that provide strong interaction with zinc cofactor through NH group of imidazole and carbonyl group of amides, aromatic linker that forming a hydrophobic interaction between aromatic rings and residues of amino acid in the grooves of protein, and bulky fused ring in CAP group that induce fitting of whole structure in the active site of HDAC enzyme. These pharmacophoric features of **K1** provide geometric and electrostatic complementarity reflect highest binding affinity and docking score. The ADME analysis for **K1** indicated an acceptable pharmacokinetic property. The MD analysis revealed that the compound **K1-**1T69 complexes were stable and have perfect protein ligand interaction along simulation time and has acceptable RMSD and RSMF value in comparable to vorinostat which reflect a good ligand interaction with HDAC8 enzymes. Chemical synthesis for the most active molecules and examine their biological activity is our future plan.

REFERENCE

1. Tronick E, Hunter RG. Waddington, Dynamic Systems, and Epigenetics. Front Behav Neurosci. 2016;10:107. https://doi.org/10.3389/fnbeh.2016.00107
2. Saeed AM, Al-Hamashi AA. Molecular Docking, ADMET Study, Synthesis, Characterization and Preliminary Antiproliferative Activity of Potential Histone Deacetylase Inhibitors with Isoxazole as New Zinc Binding Group. Iraqi Journal of Pharmaceutical Sciences. 2023 Nov 3;32(Suppl.):188-203. https://doi.org/10.31351/vol32issSuppl.pp188-203
3. Abdulameer AMS, Al-Hamashi AAA. Docking, ADMET study, Synthesis and Biological evaluation of Isoxazole Derivatives as potential Histone Deacetylase Inhibitors. History of Medicine. 2023;9(1):2501-508. https://doi.org/10.17720/2409-5834.v9.1.2023324
4. Mosa HM, Al-Hamashi AA. Design, Synthesis, and Cytotoxicity Evaluation of Sulfonamide Derivatives as Potential HDAC Inhibitors. Azerbaijan Pharmaceutical and Pharmacotherapy Journal. 2023;22(2):214-7. https://doi.org/10.61336/appj/22-2-44
5. Jones P, Issa JP, Baylin S. Targeting the cancer epigenome for therapy. Nat Rev Genet. 2016;17:630-41. https://doi.org/10.1038/nrg.2016.93
6. Al-Hamashi A, Abdulhadi S, Ali R. Evaluation of Zinc Chelation Ability for Non-Hydroxamic Organic Moieties. Egyptian Journal of Chemistry. 2023;66(5):215-21. https://doi.org/10.21608/ejchem.2022.147377.6415
7. Al-Hamashi AA, Koranne R, Dlamini S, Alqahtani A, Karaj E, Rashid MS, et al. A new class of cytotoxic agents targets tubulin and disrupts microtubule dynamics. Bioorg Chem. 2021;116:105297. https://doi.org/10.1016/j.bioorg.2021.105297
8. Alwash AH, Naser NH. Synthesis, characterization, and vitro evaluation of new materials in vorinostat analogs containing biomolecules. Materials Today: Proceedings. 2022;60:1424-39. https://doi.org/10.1016/j.matpr.2021.11.016
9. Nadendla RR. Molecular modeling: A powerful tool for drug design and molecular docking. Reson. 2004;9:51-60. https://doi.org/10.1007/BF02834015
10. Ferreira LG, Dos Santos RN, Oliva G, Andricopulo AD. Molecular Docking and Structure-Based Drug Design Strategies. Molecules. 2015;20:13384-421. https://doi.org/10.3390/molecules200713384

11. Zhu K, Borrelli KW, Greenwood JR, Day T, Abel R, Farid RS, et al. Docking Covalent Inhibitors: A Parameter Free Approach To Pose Prediction and Scoring. J Chem Inf Model. 2014;54(7):1932-40. https://doi.org/10.1021/ci500118s
12. Halgren TA, Murphy RB, Friesner RA, Beard HS, Frye LL, Pollard WT, et al. Glide: A new approach for rapid, accurate docking and scoring. J Med Chem. 2004;47:1750-59. https://doi.org/10.1021/jm030644s
13. Hai Y, Christianson D. Histone deacetylase 6 structure and molecular basis of catalysis and inhibition. Nat Chem Biol. 2016;12:741-47. https://doi.org/10.1038/nchembio.2134
14. Lauffer BE, Mintzer R, Fong R, Kaminker JS, Heise CE, Steiner P, et al. Histone deacetylase (HDAC) inhibitor kinetic rate constants correlate with cellular histone acetylation but not transcription and cell viability. J Biol Chem. 2013;288(37):26926-43. https://doi.org/10.1074/jbc.M113.490706
15. Somoza JR, Skene RJ, Katz BA, Swanson RV, McRee DE, Tari LW, et al. Structural snapshots of human HDAC8 provide insights into the class I histone deacetylases. Structure. 2004 Jul;12(7):1325-34. https://doi.org/10.1016/j.str.2004.04.012
16. Mali S, Chaudhari H. Computational Studies on Imidazo[1,2-a] Pyridine-3-Carboxamide Analogues as Antimycobacterial Agents: Common Pharmacophore Generation, Atom-based 3D-QSAR, Molecular dynamics Simulation, QikProp, Molecular Docking and Prime MMGBSA Approaches. Open Pharmaceutical Sciences Journal. 2018;5:13. https://doi.org/10.2174/1874844901805010012
17. Lu C, Wu C, Ghoreishi D, Chen W, Wang L, Damm W, et al. OPLS4: Improving force field accuracy on challenging regimes of chemical space. J Chem Theory Comput. 2021;17(7):4291-300. https://doi.org/10.1021/acs.jctc.1c00302
18. Friesner RA, Murphy RB, Repasky MP, Frye LL, Greenwood JR, Halgren TA, et al. Extra precision Glide: Docking and scoring incorporating a model of hydrophobic enclosure for protein-ligand complexes. J Med Chem. 2006;49:6177-96. https://doi.org/10.1021/jm051256o
19. QikProp, Schrödinger, LLC, New York, NY. 2021.
20. Bowers KJ, Chow E, Xu H, et al. Scalable algorithms for molecular dynamics simulations on commodity clusters. Proceedings of the ACM/IEEE Conference on Supercomputing (SC06), Tampa, Florida, November 11-17, 2006. https://doi.org/10.1145/1188455.544
21. Hasan Y, Al-Hamashi A. Identification of Selisistat Derivatives as SIRT1-3 Inhibitors by in Silico Virtual Screening. Turkish Computational and Theoretical Chemistry. 2024;8(2):1-11. https://doi.org/10.33435/tcandtc.1224592
22. Repasky MP, Murphy RB, Banks JL, Greenwood JR, Tubert-Brohman I, Bhat S, et al. Docking performance of the glide program as evaluated on the Astex and DUD datasets: a complete set of glide SP results and selected results for a new scoring function integrating WaterMap and glide. J Comput Aided Mol Des. 2012;26:787-99. https://doi.org/10.1007/s10822-012-9575-9
23. Ntie-Kang F. An in-silico evaluation of the ADMET profile of the Streptome DB database. Springerplus. 2013 Jul 30;2:353. https://doi.org/10.1186/2193-1801-2-353
24. Hollingsworth S, Dror R. Molecular Dynamics Simulation for All. Neuron. 2018;99:1129-43. https://doi.org/10.1016/j.neuron.2018.08.011

CONFLICT OF INTEREST
Authors declare no conflict of interest.
GRANT SUPPORT AND FINANCIAL DISCLOSURE
None declared.

AUTHORS' CONTRIBUTION

The following authors have made substantial contributions to the manuscript as under:

Conception or Design:	ZMM, AAAA
Acquisition, Analysis or Interpretation of Data:	ZMM, AAAA
Manuscript Writing & Approval:	ZMM, AAAA

All the authors agree to be accountable for all aspects of the work in ensuring that questions related to the accuracy or integrity of any part of the work are appropriately investigated and resolved.